HHS Public Access

Author manuscript

J Mol Biol. Author manuscript; available in PMC 2017 February 27.

Published in final edited form as:

J Mol Biol. 2016 February 27; 428(5 Pt A): 811–821. doi:10.1016/j.jmb.2015.10.009.

Predicting Large RNA-Like Topologies by a Knowledge-Based Clustering Approach

Naoto Baba[1,2], **Shereef Elmetwaly**[1], **Namhee Kim**[1], and **Tamar Schlick**[1]

[1]Department of Chemistry and Courant Institute of Mathematical Sciences, New York University, 251 Mercer Street, New York, NY, 10012

[2]Department of Chemistry, Nagoya University, Furo-cho, Chikusa-ku, Nagoya, Aichi, 464-8601 Japan

Abstract

An analysis and expansion of our resource for classifying, predicting, and designing RNA structures, RAG (RNA-As-Graphs), is presented, with the goal of understanding features of RNA-like and non-RNA-like motifs and exploiting this information for RNA design. RAG was first reported in 2004 for cataloguing RNA secondary structure motifs using graph representations. In 2011, the RAG resource was updated with the increased availability of RNA structures and improved by utilities for analyzing RNA structures, including substructuring and search tools. We also classified RNA structures as graphs up to 10 vertices (~ 200 nucleotides) as three classes: existing, RNA-like, and non-RNA-like using clustering approaches. Here, we focus on the tree graphs and evaluate the newly founded RNAs since 2011, which also support our refined predictions of RNA-like motifs. We expand the RAG resource for large tree graphs up to 13 vertices (~ 260 nucleotides), thereby cataloguing more than 10 times as many secondary structures. We apply clustering algorithms based on features of RNA secondary structures translated from known tertiary structures to suggest which large RNA motifs can be considered “RNA-like”. The results by the Partitioning Around Medoids (PAM) approach, in particular, reveal good accuracy, with small error for the largest cases. The RAG update here up to 13 vertices offers a useful graph-based tool for exploring RNA motifs and suggesting large RNA motifs for design.

Graphical abstract

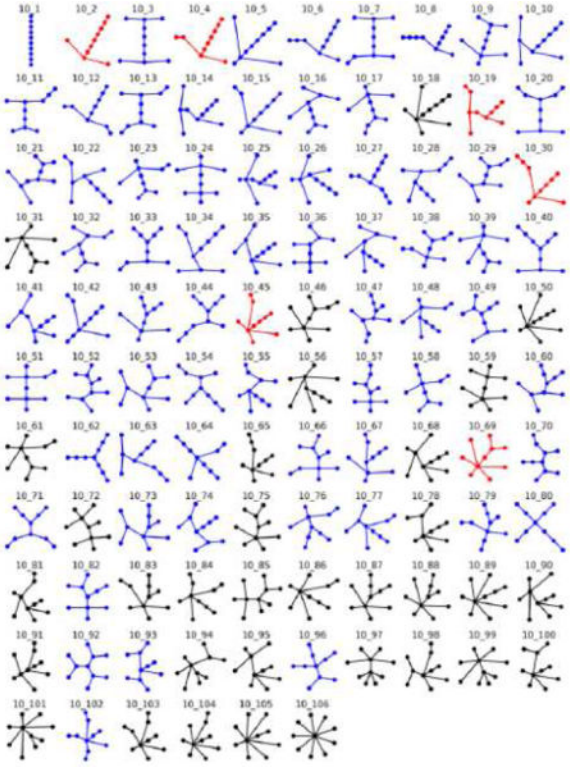

Segments of RAG Extension: Enumerated graphs of RNA secondary structures with labeling of those found in Nature(red).

Keywords

RNA secondary structure; RNA atlas; RNA motifs; RNA design; Prediction of RNA-like motifs

Introduction

It is now well appreciated that RNA molecules have essential roles in the regulation of gene expression and signal recognition[1–4] besides their widely known roles in protein synthesis by mRNA, tRNA, and rRNA. The functionalities of RNAs are made possible by large variations of secondary and tertiary motifs. Unlike proteins, where structural genomics initiatives have been advancing for decades[5,6], systematic connections between RNA structures and their biological roles remain largely unclear. Thus, improvements in the connection between RNA's structure and its functionality can help advance our understanding of RNAs as well as the design of new RNAs.

The secondary structure of RNA, less complex than its tertiary structure, is already a good starting point for a structural/functional analysis. Secondary structures, in particular, are amenable to mathematical analysis by graph theory. Graph theory is a well-established field of mathematics, which has been used extensively in a variety of economic, social, engineering, biological, and medical contexts to describe and analyze complex networks[7–10]. Shareability networks have been used recently, for example, to analyze cab

sharing in New York City and promote a 40% reduction in traffic and pollution due to simple sharing of cabs[11]. We utilize graph theory here to analyze RNA secondary structures: we transform RNA secondary structures into graph vertices and edges to express RNAs as coarse-grained objects, thereby forgoing a detailed atomic-level representation. Applying graph theory to compare the 2D graphical representations has already shown to be useful in some projects[12–14].

In 2004, we developed and launched the RNA-As-Graph (RAG) web resource (http://www.biomath.nyu.edu/rag/home). This framework catalogs all possible RNA 2D topologies up to 10 vertices and classifies them as existing or hypothetical, with the latter divided into RNA-like ("non-existing but RNA-like") and non-RNA-like ("non-existing and not RNA-like")[15], by clustering features at RNA secondary structures as tree and dual graphs by means of graph theory. The graphical information extracted is in the form of the adjacency and Laplacian matrices, which describe graph connections, and the clustering is performed by their vertex number and eigenvalue spectrum (See *Materials and Methods*).

The many applications of RAG, as reviewed recently[16–18], include the prediction of RNA-like topologies[19–22], prediction of non-coding RNA[23,24], computational modeling of the *in vitro* selection process for RNA design[25–27], analysis of large viral RNA[28,29], analysis and design of riboswitches[30,31], graph partitioning to explore RNA modularity[16,17,32], and prediction of 3D RNA topologies[33,34].

Many new RNA databases have been developed since 2004. For example, RNA family database (Rfam)[35] displays consensus secondary structures for 1,372 families of RNA[36], and the RNA Strand database catalogs 4,666 secondary structures determined by comparative sequence analysis, NMR data, and X-Ray crystallography[37]. This growth allowed us to extend RAG and propose an improved classification in 2011. In addition, we implemented various improvements to the RAG web resource such as expanded search tools and a user-friendly interface. The 2011 update was still limited to tree graphs up to 10 vertices corresponding to about 200 nucleotides of RNA sequences.

In this work, we upgrade the RAG database with new prediction results for RNA-like topologies for large tree graphs up to 13 vertices (~260 nucleotides) in length, using an auxiliary graph computation program named nauty and Traces[38]. This makes RAG's coverage more than 10 fold greater. We then catalogue new existing RNAs from the PDB database, as of Aug 2014, for all secondary structures translated from solved experimental structures. Finally, a new prediction for RNA-like motifs is described based on the Partitioning Around Medoids (PAM) clustering approach[39].

This paper is organized as follows. We begin by brief review of the conversion process from RNA secondary structures to RAG 2D graph representations. Next, the new graph enumeration scheme that allowed this significant RAG expansion is introduced, and the extraction of characteristic information from these secondary graphs is detailed. We then discuss how to choose the proper clustering method. Our main achievements consist of the two parts: high accuracy of predicted RNA-like features for the newly found RNAs, and our extended RAG for larger topologies based on the current dataset. In Discussion, we

elaborate upon the significance of those findings, and mention the future prospects of clustering for RNAs.

Materials and Methods

RNA secondary structure data

In our previous works, we used several RNA secondary structure repositories: Rfam[40], Pseudobase++[41], RNA Strand[42], Protein Databank (PDB)[43], and Nucleic Acid Database[44,45], for cataloging secondary structures that are either fully or partially evaluated by experiment. Here, to analyze the accuracy and efficiency of our RAG clustering strategy for predicting RNA-like motifs, RNA secondary structures were exclusively collected from PDB with untangling of multiple chains, so that the structures we classify are all experimentally validated. We also include pseudoknot structures, which are translated into non-pseudoknot structures for a representation as tree graphs by removal of extra base pairings composing the pseudoknots. Note that dual graphs, as we have described separately[15,46], can be used to model pseudoknotted RNA fully. A simple modification of tree graphs to model pseudoknots was also recently presented and applied for prediction of tertiary structures[18].

RNA tree graph representation

The conversion process from detailed RNA secondary structures to tree graph representations was detailed in our previous works[15,19]. Briefly, RAG considers nucleotide bulges, hairpin loops, internal loops, junctions and the 3′ and 5′ ends as vertices, and RNA stems as edges (see Figure 1).

Enumeration of RNA graphs

To classify all existing graph motifs including the experimentally found and those not yet solved experimentally, we generate all possible tree graphs with a given number of vertices. Graph theory offers enumeration methods for describing all possible graphs[47]. Previously, we had used the counting polynomial of Harary-Prins and the figures of Graph Theory[47], but this scheme for tree graphs was manual; the polynomial gives the number of the graphs but no information about the shape, or topology, of the graphs.

An alternative is the integration of nauty and Traces[38], two programs focused on canonical labeling and automorphism group computations. These programs can exhaustively produce all desired tree graphs. The completeness of the graph generation is verified by two requirements: the number of generated graphs should match the result of the counting polynomial of Harary-Prins, and there should be no isomorphic graphs, which is confirmed by NetworkX[48]. Thus, we ensure that all the non-isomorphic graphs are generated. This effective combination allows us to extend RAG significantly by adding 235, 551 and 1,301 tree graphs for 11, 12 and 13 vertices, respectively.

Topological descriptors of RNA graphs: Laplacian spectra

To order all the graphs by their features, we use the second eigenvalue λ_2 of the Laplacian matrix, a matrix which describes graph connections. The other eiganvalues are associated

with a spectral decomposition associated with the graph, useful for many applications, e.g., graph partitioning by the second eigenvector[32].

To define the Laplacian matrix, we define the $n \times n$ adjacency matrix for an n-node graph where the non-diagonal entries a_{ij} are 1 if there is an edge between vertex i and j, and 0 otherwise.

The Laplacian matrix (L) is defined by $L = D - A$, where D is the diagonal matrix whose diagonal elements a_{ii} specify the degree of connectivity of vertex i. Thus, for example, a straight-line shaped graph with 3 vertices has graph ID 3_1 in the RAG terminology, and corresponding D, A, and L matrices as follows:

$$D=\begin{pmatrix} 1 & 0 & 0 \\ 0 & 2 & 0 \\ 0 & 0 & 1 \end{pmatrix}, \quad A=\begin{pmatrix} 0 & 1 & 0 \\ 1 & 0 & 1 \\ 0 & 1 & 0 \end{pmatrix}, \quad L=D-A=\begin{pmatrix} 1 & -1 & 0 \\ -1 & 2 & -1 \\ 0 & -1 & 1 \end{pmatrix}$$

Note that the spectrum of the Laplacian matrix is independent of the labeling of graph vertices because a change in labeling can be accomplished by the elementary operations on the matrices and the elementary operations do not alter their eigenvalues. Thus, if the spectra of the Laplacian matrices of two graphs are different, the graphs are also different. Although identical spectra can be associated with different graph topologies, this situation is rare[38].

The pattern of a graph's connectivity is related to its eigenvalue spectrum (spectral graph theory)[49]. The second smallest eigenvalue, λ_2, for example, is called the algebraic connectivity and measures the graph's compactness: a linear chain has a smaller second eigenvalue than a branched structure[50]. Thus, the RNAs are analyzed by means of their graph invariants, which are eigenvalues here.

Labeling the tree graphs with IDs

We label all tree graphs of the same vertex number by increasing λ_2. Thus, for example, ID 6_1 indicates that the graph has 6 nodes and the smallest λ_2 among all 6-node graphs; ID 6_3 indicates the 6-node graph with the third lowest λ_2, and so on.

Deduction of characteristic information from the Laplacian spectra

To derive essential topological features of an RNA graph so we can compare and visualize, in 2D or 3D, the graphs with varying number of nodes, we compress the number of descriptors from the Laplacian spectrum, which is composed of n eigenvalues for a graph of n vertices, to two variables α and β: the slope α and the intercept β are calculated by applying the linear least-square regression to the set of planar points (1, λ_2), (2, λ_3), …, (n − 1, λ_n). The first eigenvalue λ_1 is omitted because its value is always zero. Thus, α measures the average spacing between positive eigenvalues and the intercept β represents the second smallest eigenvalue calibrated by α. This type of reduction mechanism is commonly used in clustering analysis. One example is in the field of drug design, known as quantitative structure-activity relationships (QSAR)[51], where various chemical compounds are described by a few 'topological descriptors'.

Here we observe that a decreases with n, and therefore, we assume that na forms a quantity independent of n. We thus derive a set of two descriptors, (na, β), and use this quantity as a component to perform clustering of RNA-like and non-RNA-like motifs based on the existing RNA databases. In addition, considering the relationship of the eigenequation for powers k = 0, 1, 2, …,

$$L^k x_i = \lambda_i^k x_i \, (i = 1, 2, \ldots, n),$$

where x_i is an eigenvector corresponding to λ_i, enhances the accuracy of clustering effectively[15] by allowing us to add more parameters. We define a_k and β_k in the same manner from the powers of the eigenvalues $(1, \lambda_2^k), (2, \lambda_3^k), \ldots, (n-1, \lambda_n^k)$. Thus, a point in a $2k$ dimensional space is obtained for each secondary structure. Our previous work[15] showed some advantage of the k=2 space over other values, so this value is consistently used here too.

To make each coordinate's contribution equal for the predictions, these values are normalized based on the average of their absolute values. That is, if we let x_m = (mth coordinate), e.g., $x_1 = na_1$, the normalized coordinates x_m^* are

$$x_m^* = (\overline{x_1}/\overline{x_m}) x_m.$$

Note that, although we chose ($\overline{x_1}$) for the numerator, this could be the mean of any x_m.

Finally, the metric multidimensional scaling (MDS) is performed to map these 4 dimensional points to the same number of 2 dimensional points keeping the Euclidean distances among the original points as much as possible[52].

Clustering and Validation Procedure

Overall, our goal is to predict which of the hypothetical tree graphs are RNA-like. To do so, the data points generated from the tree graphs are clustered into 2 categories: RNA-like and non-RNA-like. Two very different clustering approaches can be considered: k-nearest neighbor (k-NN)[53,54] and partitioning around medoids (PAM)[39]. The former use training data while the latter does not.

The k-NN algorithm classifies a point based on k closest training data points: A point is classified by a majority vote of its neighbors, with the point being assigned to the class most common among its k nearest neighbors[53,54]. However, due to the lack of existing motifs for higher vertices, we use all existing motifs and the same number of randomly selected non-existing motifs as a training set. Because of this randomness, we employed 10 trials by varying the set of random non-existing data.

Once a training set is given, cross-validation is one of several approaches for estimating how well the model might perform on future data. One effective cross-validation method is called leave-one-out cross validation (LOOCV)[55]. As its name suggests, LOOCV leaves one data

item from the training set and performs a clustering to this single isolated data point by the training set which now lacks that item. This process is repeated for each data item, and the reliability of the prediction is measured by comparison to confirmed RNA-like and non-RNA-like motifs.

PAM, on the other hand, requires no training set. PAM partitions all data (existing and hypothetical graph features) in an 'ab initio' manner to predict two groups (RNA-like and non-RNA-like) that are maximally separated[39]. Thus, PAM clusters the data into these two groups, each with its center or medoid, by minimizing the distances within groups and maximizing the distance between groups.

The fact that the PAM requires no training set makes the validation fairly straightforward. We simply perform PAM clustering on the current dataset and calculate the accuracy naturally by

$$\frac{(\text{Total number of existing RNAs predicted correctly as RNA- like})}{(\text{Number of known existing RNAs})}.$$

We further check and confirm actual existing RNAs predicted as either RNA-like or non-RNA-like graphs (i.e., that we get not just the right number but the right graphs).

Program Implementation

As mentioned, the 2D tree graphs are generated by the combination of nauty and Traces[38] and NetworkX[48]. The code for converting RNA 2D full topology to a tree graph, which was described in the section *RNA tree graph representation*, was automated in our previous work[19] and is used here too. The MDS is done by the implementation of the function *cmdscale* from the multivariable analysis library package of R[56]. The *k*-NN and PAM clustering are performed by The C clustering library[20]. All other parts are coded by the first author using Python. The entire calculation process takes less than 2 hours on Intel® Core™ i5-4258U.

Results

Association of secondary structures to new RNAs

The process of converting an RNA 2D full topology to a tree graph, which was described in the section *RNA tree graph representation*, is automated in RAG[19]. This allowed us to exhaustively inspect the current RNA structures and assign a secondary graph motif to each. Taking RNA structures from Protein Data Bank (PDB) yielded Figure 2. Many new topologies were identified, even from the RNAs that had been identified before our last work, because our current procedure for excision of pseudoknots and separation of multiple chains allows the conversion of the RNA structures that could not be handled previously as tree graphs.

Clustering assessment by the current status

Early in our RAG project, the two clustering methods, Partitioning Around Medoids (PAM)[39] and *k*-nearest neighbor (*k*-NN)[53,54] were used for predicting novel RNA topologies based on clustering. Because *k*-NN considers randomized data for its prediction, we consider it now to be less reliable than PAM.

Indeed, by the procedure described above (*Clustering and Validation Procedure*), we obtain 77.27% accuracy from PAM (Figure 3 and Table 1) compared to poorer results by *k*-NN (see Supplemental Material).

High accuracy of RAG prediction on the newly found RNAs

The PAM clustering method classifies the motifs associated with the newly found RNAs as in Table 2, as shown in Figure 3 Many of the newly found RNAs were categorized as RNA-like by the RAG clustering strategy. Notably, although three motifs were misclassified as non-RNA-like, they all have only one existing RNA; the motifs that have multiple existing RNAs were all correctly classified as RNA-like.

The RNAs that are misclassified are the following: RNA component of bacterial ribonuclease P (PDB ID 2A2E, chain A)[57]; adenosylcobalamin riboswitch (PDB ID 4GMA, chain Z)[58]; tmRNA-SmpB ribonucleoprotein complex (PDB ID 3IYR, chain A)[59].

Drastically extended RAG for larger topologies and its accuracy based on the current dataset

The number of vertices for RNAs is not limited to 10 because nauty and Traces can generate secondary graphs with more vertices. By integrating this software with our program, all tree graphs through 13 vertices were exhaustively created, which allows the enumeration of much larger sets of topological descriptors. Thus, RAG has extended its coverage by more than 10 fold; RAG in 2011 catalogued 199 secondary graph motifs, but now the count is 2,286, with 2,087 graph motifs added. Since the graph motifs with varying numbers of nodes are clustered together in RAG, we can make RNA-like predictions for larger topologies regardless of the lack of larger existing motifs. Such predictions can be evaluated based on the RNAs archived from the PDB, which includes new RNAs in addition to the others that we could not represent in 2011. The result is shown as Table 1. The result for 11 vertices is somewhat poor, but there is only one misclassified data for 13 vertices, and there is no error for 12 nodes. There is only one graph, RAG ID 11_24, with multiple existing RNAs, and it is predicted properly as RNA-like. Table 1 also shows the statistics for higher vertices, and Figure 4 visualizes the counts of existing RNA-like and existing misclassified non-RNA-like in Table 1.

Finally, a complete catalog of our RAG data was provided. Because of space limitations, only a subset is shown in Figure 5 for 10-vertex graphs. The full catalog can be found in the Supplemental Material and on our RAG website (http://www.biomath.nyu.edu/rag/home)

Discussion

We have extensively updated our RAG database based on the newly discovered RNA structures using our computer program by deploying the exhaustively enumerated RAG motifs represented as tree graphs. Our clustering results show two significant gains: the RAG clustering strategy yields near 80% accuracy for predicting existing-RNA topologies, and no motif with multiple existing RNA structures is misclassified. Thus, estimating features of RNA-like structures according to their topological representation may be a powerful strategy for RNA design. The predicted RNA-like candidates are good design candidates, as already suggested. [15,16,19]

In our previous work[15], we used a build-up approach to predict and identify sequences that fold onto ten candidate dual graph motifs. Among those ten candidate motifs, five have since been experimentally determined.[16,19] To design RNA sequences that fold onto the targeted RNA-like topologies, we have used graph partitioning algorithms based on Laplacian eigenvectors[32]. We recently suggested a gap cut approach which partitions a graph into two graphs by the largest gap of the sorted second Laplacian eigenvector μ_2; we have illustrated how to use this gap cut partitioning to describe basic modules of RNAs and propose their hierarchical assembly[32].

Figure 6 sketches a design application for RNA-like graphs. Here we aim to design a large RNA-like graph, RAG ID 11_205. The gap cut suggests partitioning the graph 11_205 into two substructures, an existing 5_3 corresponding to tRNA (PDB ID: 2DU3) and an RNA-like 7_4 graph. The latter graph is further partitioned into two identical existing graphs 4_2 corresponding to the hammerhead riboyzme (PDB ID: 1RMN). The assembly of these existing sequences provides a starting candidate sequence for the large RNA corresponding to the target RNA-like graph 11_205. Of course, computational refinement by 2D structure prediction programs, not to speak of thermodynamic and experimental verifications, are needed for confirmation. Yet this systematic design protocol for novel RNA-like topologies could help expand the structural and functional repertoire of RNAs.

Although the RAG classification and prediction described here exhibited good accuracy for predicting existing RNA topologies, many improvements can be envisioned. In addition to eigenvalues, Laplacian eigenvectors could also be useful for graph descriptors. The second eigenvector was shown to be useful for graph partitioning for the discovery of RNA modularity[32]. This kind of approach reveals a connection between RNAs' higher order structures and their properties. A challenge for the future is to integrate other descriptors and other methods with the current strategy to improve the results.

Conclusion

Focusing on tree graphs, our refined RAG classification method was shown to predict well RNA-like and non-RNA-like topologies of secondary structures with near 80% accuracy. We have also expanded the database significantly to larger topologies, adding 10 times as many topologies since the last update. Our analysis suggests that a topology prediction

approach can be productive and reinforces the idea that the properties of RNAs can be analyzed to a first approximation by means of their secondary structures.

Supplementary Material

Refer to Web version on PubMed Central for supplementary material.

Acknowledgments

This work is supported by the National Science Foundation (DMS-0201160, CCF-0727001) and the National Institute of Health (GM100469, GM081410). Naoto Baba also would like to thank Professor Irle at Nagoya University for his support. We also thank Cigdem S. Bayrak for her assistance.

References

1. Eddy SR. Non-coding RNA genes and the modern RNA world. Nat Rev Genet. 2001; 2:919–929. [PubMed: 11733745]
2. Nudler E. Flipping Riboswitches. Cell. 2006; 126:19–22. [PubMed: 16839869]
3. Breaker RR. Riboswitches and the RNA World. Cold Spring Harb Perspect Biol. 2010; 4(2):a003566. [PubMed: 21106649]
4. Gribaldo S, Brochier-Armanet C. The origin and evolution of Archaea: a state of the art. Philos Trans R Soc Lond B Biol Sci. 2006; 361:1007–1022. [PubMed: 16754611]
5. Burley SK, et al. Structural genomics: beyond the Human Genome Project. Nature Genet. 1999; 23:151–157. [PubMed: 10508510]
6. Chance MR, et al. Structural genomics: A pipeline for providing structures for the biologist. Protein Sci. 2002; 11:723–738. [PubMed: 11910018]
7. Bray D. Molecular Networks: The Top-Down View. Science. 2003; 301:1864–1865. [PubMed: 14512614]
8. Kalir S, Alon U. Using a Quantitative Blueprint to Reprogram the Dynamics of the Flagella Gene Network. Cell. 2004; 117:713–720. [PubMed: 15186773]
9. Barabási AL, Bonabeau E. Scale-Free Networks. Sci Am. 2003; 288:60–69. [PubMed: 12701331]
10. Yook SH, Jeong H, Barabási AL. Modeling the Internet's large-scale topology. Proc Natl Acad Sci USA. 2002; 99:13382–13386. [PubMed: 12368484]
11. Santi P, et al. Quantifying the benefits of vehicle pooling with shareability networks. Proc Natl Acad Sci USA. 2014; 111:13290–13294. [PubMed: 25197046]
12. Le SY, Nussinov R, Maizel JV. Tree graphs of RNA secondary structures and their comparisons. Comput Biomed Res. 1989; 22:461–473. [PubMed: 2776449]
13. Benedetti G, Morosetti S. A graph-topological approach to recognition of pattern and similarity in RNA secondary structures. Biophys Chem. 1996; 59:179–184. [PubMed: 8867337]
14. Fontana W, Konings DAM, Stadler PF, Schuster P. Statistics of RNA Secondary Structures. Biopolymers. 1993; 33:1389–1404. [PubMed: 7691201]
15. Kim N, Shiffeldrim N, Gan HH, Schlick T. Candidates for Novel RNA Topologies. J Mol Biol. 2004; 341:1129–1144. [PubMed: 15321711]
16. Kim, N.; Fuhr, N.; Schlick, T. Graph Applications to RNA Structure and Function. In: Russell, R., editor. Biophysics of RNA folding. Vol. 3. Springer Verlag; 2013. p. 23-51.Chapter 3Biophysics for the Life Sciences
17. Kim N, Petingi L, Schlick T. Network Theory Tools for RNA Modeling. WSEAS Transaction on Math. 2013; 12:941–955.
18. Kim N, Zahran M, Schlick T. Computational Prediction of Riboswitch Tertiary Structures Including Pseudoknots by RAGTOP: A Hierarchical Graph Sampling Approach. Methods Enzymol. 2015; 553:115–135. [PubMed: 25726463]
19. Izzo JA, Kim N, Elmetwaly S, Schlick T. RAG: An update to the RNA-As-Graphs resource. BMC Bioinformatics. 2011; 12:219. [PubMed: 21627789]

20. de Hoon, M.; Imoto, S.; Miyano, S. Inst of Medical Sci Human Genome Cent. Univ. of Tokyo; Tokyo: 2005. The C clustering library.
21. Haynes T, Knisley D, Seier E, Zou Y. A quantitative analysis of secondary RNA structure using domination based parameters on trees. BMC Bioinformatics. 2006; 7:108. [PubMed: 16515683]
22. Koessler DR, Knisley DJ, Knisley J, Haynes T. A Predictive Model for Secondary RNA Structure Using Graph Theory and a Neural Network. BMC Bioinformatics. 2010; 11(Suppl6):S21. [PubMed: 20946605]
23. Hamada M, Tsuda K, Kudo T, Kin T, Asai K. Mining frequent stem patterns from unaligned RNA sequences. Bioinformatics. 2006; 22:2480–2487. [PubMed: 16908501]
24. Laserson U, Gan HH, Schlick T. Predicting candidate genomic sequences that correspond to synthetic functional RNA motifs. Nucleic Acids Res. 2005; 33:6057–6069. [PubMed: 16254081]
25. Kim N, Shin JS, Elmetwaly S, Gan HH, Schlick T. RAGPools: RNA-As-Graph-Pools—a web server for assisting the design of structured RNA pools for in vitro selection. Bioinformatics. 2007; 23:2959–2960. [PubMed: 17855416]
26. Kim N, Izzo JA, Elmetwaly S, Gan HH, Schlick T. Computational generation and screening of RNA motifs in large nucleotide sequence pools. Nucleic Acids Res. 2010; 38:e139. [PubMed: 20448026]
27. Kim N, Gan HH, Schlick T. A computational proposal for designing structured RNA pools for in vitro selection of RNAs. RNA. 2007; 13:478–492. [PubMed: 17322501]
28. Gopal A, Zhou ZH, Knobler CM. Visualizing large RNA molecules in solution. RNA. 2012; 18:284–299. [PubMed: 22190747]
29. Bakhtin Y, Heitsch CE. Large Deviations for Random Trees and the Branching of RNA Secondary Structures. Bulletin of Mathematical Biology. 2009; 71:84–106. [PubMed: 19083065]
30. Quarta G, Kim N, Izzo JA, Schlick T. Analysis of Riboswitch Structure and Function by an Energy Landscape Framework. J Mol Biol. 2009; 393:993–1003. [PubMed: 19733179]
31. Quarta G, Sin K, Schlick T. Dynamic Energy Landscapes of Riboswitches Help Interpret Conformational Rearrangements and Function. PLoS Comput Biol. 2012; 8:e1002368. [PubMed: 22359488]
32. Kim N, Zheng Z, Elmetwaly S, Schlick T. RNA Graph Partitioning for the Discovery of RNA Modularity: A Novel Application of Graph Partition Algorithm to Biology. PLoS One. 2014; 9:e106074. [PubMed: 25188578]
33. Kim N, Laing C, Elmetwaly S, Jung S, Curuksu J, Schlick T. Graph-based sampling for approximating global helical topologies of RNA. Proc Natl Acad Sci USA. 2013; 111:4079–4084. [PubMed: 24591615]
34. Laing C, Jung S, Kim N, Elmetwaly S, Zahran M, Schlick T. Predicting Helical Topologies in RNA Junctions as Tree Graphs. PLoS One. 2013; 8:e71947. [PubMed: 23991010]
35. Gardner PP, et al. Rfam: updates to the RNA families database. Nucleic Acids Res. 2009; 37(Suppl 1):D136–D140. [PubMed: 18953034]
36. Jones SG, Bateman A, Marshall M, Khanna A, Eddy SR. Rfam: an RNA family database. Nucleic Acids Res. 2003; 31:439–441. [PubMed: 12520045]
37. Andronescu M, Bereg V, Hoos HH, Condon A. RNA STRAND: The RNA Secondary Structure and Statistical Analysis Database. BMC Bioinformatics. 2008; 9:340. [PubMed: 18700982]
38. McKay BD, Piperno A. Practical Graph Isomorphism, II. J Symbolic Computation. 2013; 60:94–112.
39. Kaufman, L.; Rousseeuw, PJ. Finding groups in data an introduction to cluster analysis. Hoboken, NJ: Wiley-Interscience; 1990.
40. Nawrocki EP, Burge SW, Bateman A, Daub J, Eberhardt RY, Eddy SR, Floden EW, Gardner PP, Jones TA, Tate J, Finn RD. Rfam 12.0: updates to the RNA families database. Nucleic Acids Res. 2015; 43(Database issue):D130–7.10.1093/nar/gku1063 [PubMed: 25392425]
41. van Batenburg FHD, Gultyaev AP, Pleij CWA, Ng J, Oliehoek J. PseudoBase: a database with RNA pseudoknots. Nucleic Acids Res. 2000; 28:201–204. [PubMed: 10592225]
42. Andronescu M, Bereg V, Hoos HH, Condon A. RNA STRAND: the RNA secondary structure and statistical analysis database. BMC Bioinformatics. 2008; 13(9):340. [PubMed: 18700982]

43. Berman HM, et al. The Protein Data Bank. Nucleic Acids Res. 2000; 28:235–242. [PubMed: 10592235]
44. Berman HM, et al. The Nucleic Acid Database: A Comprehensive Relational Database of Three-Dimensional Structures of Nucleic Acids. Biophys J. 1992; 63:751–759. [PubMed: 1384741]
45. Narayanan BC, et al. The Nucleic Acid Database: new features and capabilities. Nucleic Acids Res. 2013; 42:D114–D122. [PubMed: 24185695]
46. Petingi L, Kim N, Schlick T. Identifying and analyzing RNA pseudoknots based on graph-theoretical properties of dual graphs: a partitioning approach. 2015 In preparation.
47. Harary, F. Graph theory. Reading, Mass: Perseus Books; 1999.
48. Hagberg, AA.; Schult, DA.; Swart, PJ. Exploring network structure, dynamics, and function using NetworkX. Proceedings of the 7th Python in Science Conference (SciPy2008); 2008.
49. Brouwer, AE.; Haemers, WH. Spectra of graphs. New York, NY: Springer; 2012.
50. Chung, F. Spectral graph theory. Providence, R.I: Published for the Conference Board of the mathematical sciences by the American Mathematical Society; 1997.
51. Schlick, T. Molecular modeling and simulation an interdisciplinary guide. New York: Springer; 2002.
52. Borg, I.; Groenen, PJF. Modern multidimensional scaling theory and applications. 2. New York: Springer; 2005.
53. Ripley, BD. Pattern recognition and neural networks. Cambridge: Cambridge University Press; 1996.
54. Venables, WN.; Ripley, BD. Modern applied statistics with S. 4. New York: Springer; 2002.
55. Torgo, L. Data mining with R: Learning with case studies. Boca Raton: Chapman & Hall/CRC; 2011.
56. R Development Core Team. R: A Language and Environment for Statistical Computing. Vienna, Austria: the R Foundation for Statistical Computing; 2011.
57. Larios AT, Swinger KK, Krasilnikov AS, Pan T, Mondragon A. Crystal structure of the RNA component of bacterial ribonuclease P. Nature. 2005; 437:584–587. [PubMed: 16113684]
58. Johnson JE, Reyes FE, Polaski JT, Batey RT. B12 cofactors directly stabilize an mRNA regulatory switch. Nature. 2012; 492:133–137. [PubMed: 23064232]
59. Weis F, et al. tmRNA-SmpB: a journey to the centre of the bacterial ribosome. EMBO J. 2010; 29:3810–3818. [PubMed: 20953161]

Highlights

- RNA-As-Graphs (RAG) resources updated and expanded
- Motifs for larger RNA structures (up to about 260 nucleotides) are classified, with known RNAs indicated
- RNA-like motifs for non-existing RNAs are predicted using a clustering approach
- Prediction accuracy of clustering approach is good (~77%)
- The combined approach can suggests new RNA motif candidates for design

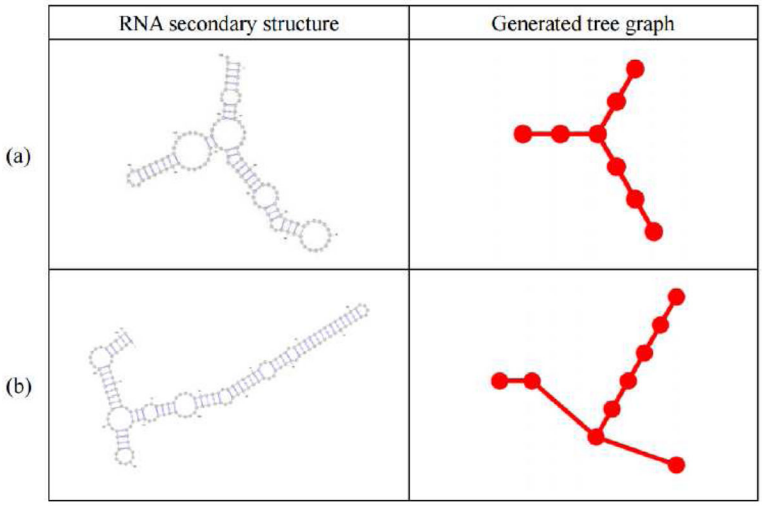

Figure 1. Conversion from a secondary RNA structure to a planar tree graph

(a) 16S ribosomal RNA (PDB ID 3J12, chain A) with its tree graph. (b) 80S ribosomal RNA (PDB ID 3IZD, chain A) with its tree graph.

Figure 2a

Graph ID	RAG motif	RNA 2D Structure	RNA (PDB ID)
8_15		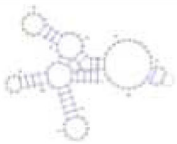 (1NBS_A)	Ribonuclease P RNA (1NBS_A), 18S ribosomal RNA (3J16_K)
9_2		(1GID_A)	Group I Intron (1GID_A, 1GID_B, 1HR2_B)
9_4		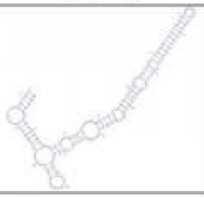	80S ribosomal RNA (3IZD_A)
9_19		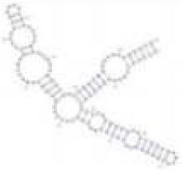 (1L9A_B)	Signal Recognition Particle (1L9A_B, 1MFQ_A, 2GO5_A, 2J37_A)

Figure 2b

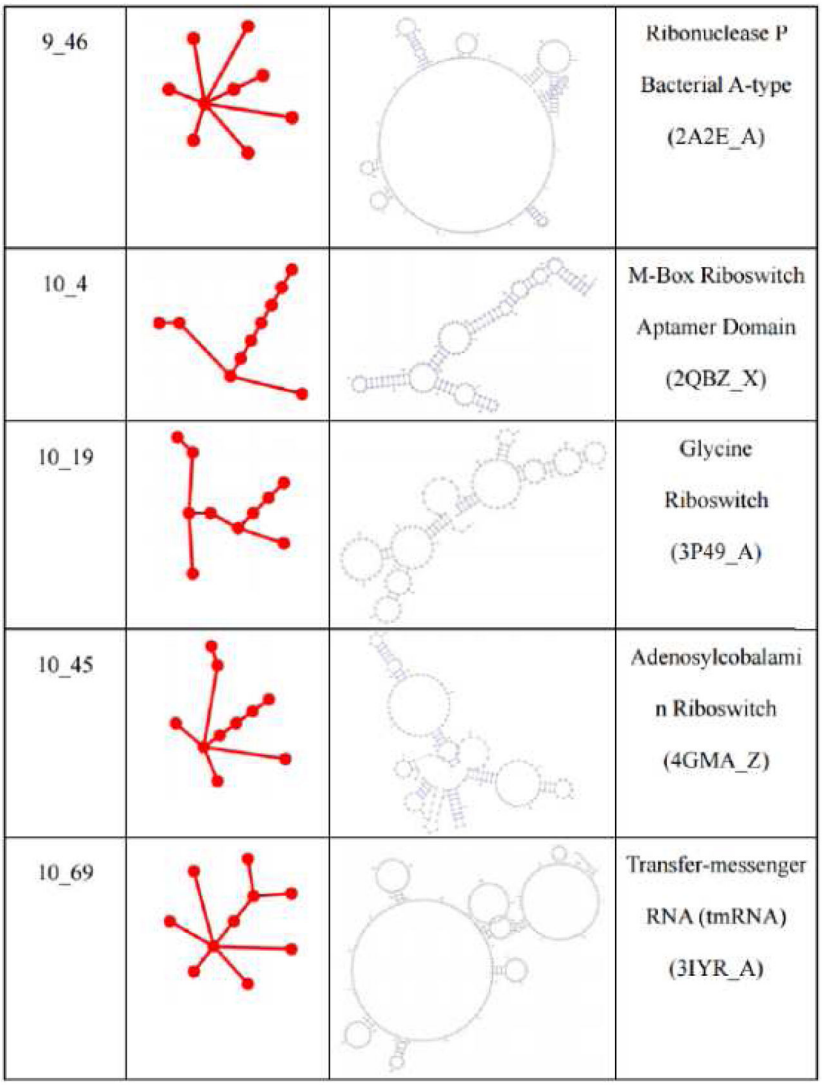

Figure 2. List of newly found motifs and their associated secondary structures of RAG graphs
For up through 10-vertex graphs, 9 new motifs have been found since our last update.

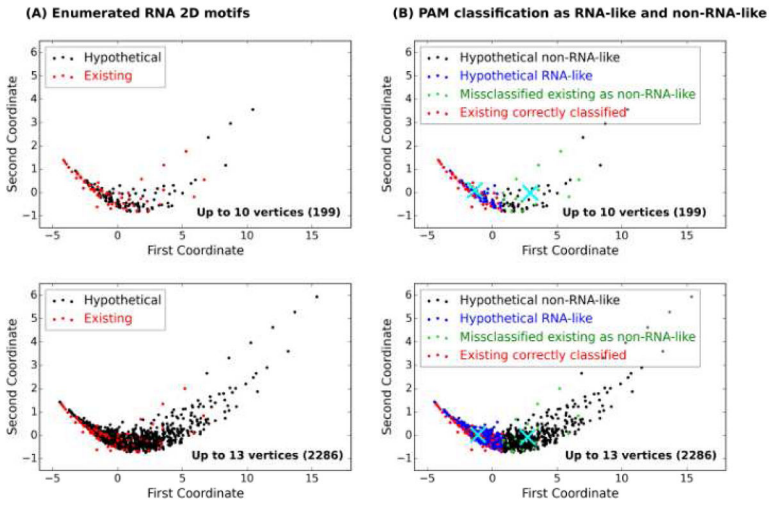

Figure 3. Plot of PAM clustering result

(A) Enumerated RNA 2D motifs up to 10 vertices (upper) and 13 vertices (lower): the x- and y-axis are the variables reduced by the MDS as described in *Deduction of characteristic information from the Laplacian spectra*. Red indicate existing RNAs. (B) PAM classification as RNA-like and non-RNA-like up to 10 vertices (upper) and 13 vertices (lower): the two medoids, or centers, of PAM are indicated by X. Most existing RNAs (65 of 84 existing RNAs) are confirmed as the RNA-like group (red) but 19 are classified as non-RNA-like (green). Hypothetical RNAs are further divided and predicted into RNA-like (blue) and non-RNA-like (black) by the PAM clustering approach.

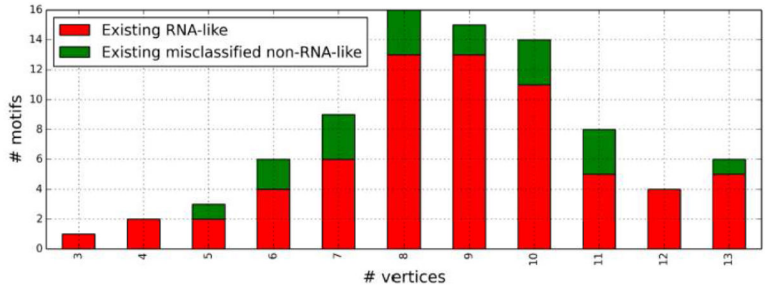

Figure 4. Numbers of existing RNA-like and existing non-RNA-like vs number of vertices

This pictorial view of the statistics obtained in Table 1 and Table 2 reveals that there are more existing RNA-like (properly predicted) topologies than existing misclassified non-RNA-like (incorrectly predicted) topologies for every number of vertices.

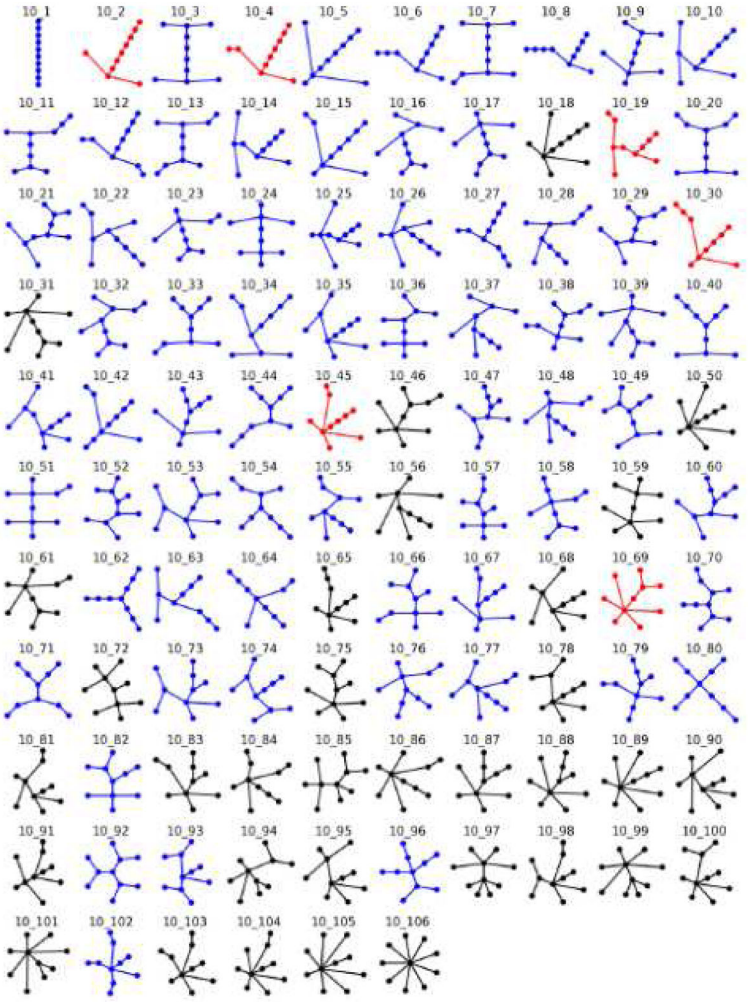

Figure 5. Illustrative subset of the RAG catalogue

We classify all enumerated graph motifs as existing, RNA-like and non-RNA-like motifs. Existing motifs are colored in red, RNA-like in blue and non-RNA-like in black. The complete version is available in Supplemental Material or http://www.biomath.nyu.edu/rag/home.

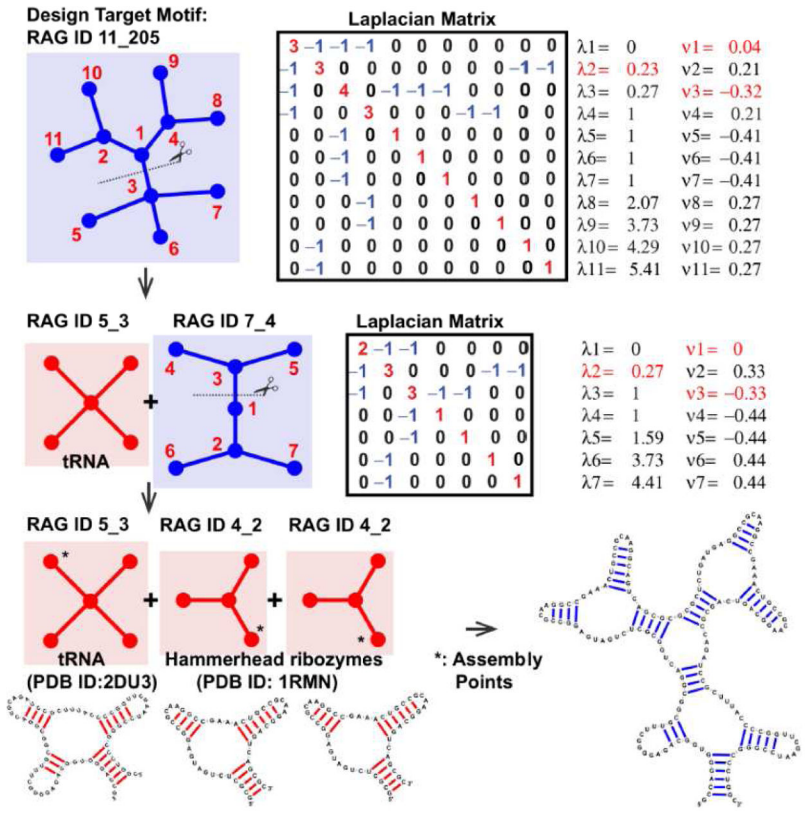

Figure 6. Design application for RNA-like topologies (example target: RAG ID 11_205)

The design procedures using graph partitioning and build-up approaches are shown. In the first row, graph 11_205 (with random vertex numbering), corresponding Laplacian matrix, eigenvalues (λ_2 in red), and the second eigenvector (μ_2) are shown. The largest gap of the sorted elements of μ_2 (vertices 1 and 3) is marked in red. In the second row, two subgraphs (existing graph 5_3 and RNA-like graph 7_4) and gap cut analysis of RNA-like graph 7_4 are shown. The third row shows the assembly procedure: the build-up of three existing modules at the assembly points suggested by gap partitioning produce a candidate RNA with the targeted graph 11_205.

Table 1

Statistics from PAM. Existing and hypothetical RNA tree motifs, each divided into RNA-like and non-RNA-like by the PAM clustering approach (see Figure 1 and Figure 3)

For the 2286 motifs up to 13 vertices, 65 are predicted correctly as RNA-like but 19 are false positives.

Vertex	Known		Predicted				Total
	Existing	Hypothetical	Existing		Hypothetical		
			RNA-like (correct class)	Non-RNA-like (misclassification)	RNA-like	Non-RNA-like	
3	1	0	1	0	0	0	1
4	2	0	2	0	0	0	2
5	3	0	2	1	0	0	3
6	6	0	4	2	0	0	6
7	9	2	6	3	2	0	11
8	16	7	13	3	4	3	23
9	15	32	12	3	21	11	47
10	14	92	11	3	60	32	106
11	8	227	5	3	156	71	235
12	4	547	4	0	391	156	551
13	6	1295	5	1	934	361	1301
Total	84	2202	65	19	1568	634	2286

Table 2
Newly found RNA motifs and their prediction classes

For motifs less than or equal to 10 vertices, motifs include updates since our 2011 RAG version. For motifs larger than 10 vertices, motifs are new. Many of the newly found graph motifs are classified as RNA-like. A few of them are misclassified as non-RNA-like, but those motifs only have a single RNA each. For example, there are 4 RNAs found for ID 9_4, which are RNA-like, but only 1 for ID 9_46, which is non-RNA-like. The larger RNA motifs more than 11 vertices include only new data. Although there are some misclassified data for 11 vertices, the other results for 12 and 13 nodes are very good. Only one RNA graph, 11_24, has 2 RNAs, and it is properly predicted as RNA-like.

Graph ID	Label	RNA (PDB ID)
8_15	RNA-like	Ribonuclease P RNA (1NBS_A), 18S ribosomal RNA (3J16_K)
9_2	RNA-like	Group I Intron (1GID_A,1GID_B,1HR2_B)
9_4	RNA-like	80S ribosomal RNA (3IZD_A)
9_19	RNA-like	Signal Recognition Particle (1L9A_B,1MFQ_A,2GO5_A,2J37_A)
9_46	non-RNA-like	Ribonuclease P Bacterial A-type (2A2E_A)
10_4	RNA-like	M-Box Riboswitch Aptamer Domain (2QBZ_X)
10_19	RNA-like	Glycine Riboswitch (3P49_A)
10_45	non-RNA-like	Adenosylcobalamin Riboswitch (4GMA_Z)
11_1	RNA-like	23S ribosomal RNA (3J5S_A)
11_24	RNA-like	M-box riboswitch (3PDR_A,3PDR_X)
11_56	RNA-like	Ribonuclease P (1U9S_A)
11_89	non-RNA-like	Transfer-messenger RNA (3IYQ_A)
11_138	RNA-like	Group 1 Intron (3BO4_B)
11_177	RNA-like	Ribonuclease P (1NBS_B)
11_207	non-RNA-like	RNase P (3DHS_A)
11_216	non-RNA-like	Group I intron with a tyrosyl-tRNA synthase (2RKJ_C)
12_150	RNA-like	tetrahymena ribozyme (1GRZ_A)
12_286	RNA-like	80S ribosomal RNA (3ZEX_E)
12_387	RNA-like	Group I intron (3IIN_B)
12_392	RNA-like	Group I intron (3BO2_BCDE)
13_140	RNA-like	Adenosylcobalamin riboswitch (4GXY_A)
13_181	RNA-like	tetrahymena ribozyme (1GRZ_B)
13_1021	RNA-like	Group I intron (1U6B_CDB)
13_1047	RNA-like	Group I intron (3BO3_CDB)

Graph ID	Label	RNA (PDB ID)
13_1154	non-RNA-like	Group I intron-product complex (1Y0Q_A)
13_1213	RNA-like	28S ribosomal RNA (3J16_J)